Transportation Research Part A 175 (2023) 103754

Contents lists available at ScienceDirect

Transportation Research Part A

journal homepage: www.elsevier.com/locate/tra

Simulation-based policy analysis: The case of urban speed limits

Qing-Long Lu [a], Moeid Qurashi [b], Constantinos Antoniou [a,*]

[a] Chair of Transportation Systems Engineering, Technical University of Munich, Munich, Germany
[b] Chair of Transport Modeling and Simulation, Technical University of Dresden, Dresden, Germany

ARTICLE INFO

Keywords:
Speed limit
Road safety
Traffic efficiency
Environmental externalities
Evidence-based policymaking

ABSTRACT

Speed limit policies are commonly adopted to manage and control traffic in urban areas due to their effectiveness and ease of implementation. Comprehending the complete effect of a speed limit policy is complicated and requires modeling and quantified investigations. In this paper, we propose a comprehensive simulation-based framework to assess the potential implications of different speed limit policies in urban residential areas. The framework models the policy impacts related to road safety (risk exposure for pedestrians and driving safety), traffic efficiency (travel time) and the environment (fuel consumption, exhaust emissions and noise exposure), using microscopic traffic simulation. The evaluations are conducted at various spatial granularity levels, i.e., link level, route level, origin–destination (OD) level and network level, and can be further utilized to develop relationship models between the key performance indicators (KPIs) and simulation inputs. The framework is implemented in an urban area located in the city center of Munich, Germany, and multiple speed limit scenarios are designed and compared. The results show that speed limit reduction can significantly improve road safety and environmental externalities within the modeled network/area with a relatively small cost to traffic efficiency. Such a framework can be used as an economical evidence collection method for an evidence-based policymaking approach to speed limit policies. The proposed simulation-based framework can also be further extended to adapt the assessment of other traffic-related policies.

1. Introduction

In most cases, policies should only be enacted after obtaining sufficient supporting evidence from experiments or analyses. This is consistent with the concept of evidence-based policymaking. While the appearance of this concept can be traced back to the fourteenth century, its absence in the practice of many domains, however, has been long lamented (Banks, 2010). Among others, the difficulty in collecting field data hinders the application of evidence-based policymaking to transport policy initiatives. Specifically, due to network connectivity and traffic flow propagation, the policy piloted in a small region could also impose a considerable impact on the entire transportation system. Therefore, it is clearly impractical to collect field data and evidence resulting from different policy scenarios through a trial-and-error approach in order to tailor the relevant provisions of the policy. Fortunately, traffic simulation provides an economical alternative to address this challenge. Modifying simulation parameters or embedding corresponding control algorithms allow one to produce simulated traffic data for the concerning transport policy environment. The potential impacts of different policy scenarios can then be estimated using the simulated data so as to provide evidence to finalize the initiative.

* Corresponding author.
E-mail addresses: qinglong.lu@tum.de (Q.-L. Lu), moeid.qurashi@tu-dresden.de (M. Qurashi), c.antoniou@tum.de (C. Antoniou).

https://doi.org/10.1016/j.tra.2023.103754
Received 7 December 2021; Received in revised form 15 June 2023; Accepted 18 June 2023
Available online 8 July 2023

With the increase in car ownership and population density, traffic-related accidents occur more frequently in cities. In addition to threatening the safety of traffic participants, non-recurrent congestion events triggered by accidents also cause a tremendous loss in social economy (Hallenbeck et al., 2003; Sun et al., 2017). For example, in 2019, the total travel delay and congestion cost of the US reached 8.7 billion hours and 190 billion dollars respectively (Lasley, 2021). Hence, traffic safety management within the urban area is always a major concern for the local government. To date, various proprietary instruments have been proposed to curb the frequency of traffic accidents, which include policies (e.g., speed limit regulation), physical measures (e.g., speed humps), economic instruments (e.g., insurance), safety education, etc. (Delhaye, 2006). Among others, speed limit policies are adopted pervasively given their effectiveness and ease of implementation.

Traffic speed is recognized as the main factor determining the frequency and severity of traffic accidents within urban areas. To be specific, higher average speeds and greater speed variances tend to produce more accidents and fatalities (Renski et al., 1999; De Pauw et al., 2014; Vadeby and Forsman, 2018). Speed limit reduction, as a policy instrument designed to reduce exposure to the risk of accidents, is capable of reducing average speed and homogenizing the traffic flow (Di Costanzo et al., 2020). Apart from improving road safety, speed limit reduction also imposes an influence on traffic efficiency and environmental externalities. In terms of traffic efficiency, on the one hand, it can promote the alleviation of traffic congestion and homogenization of traffic flow. On the other hand, it also slows down the vehicles on the enforced roads. It means that the effect on traffic efficiency is not straightforward and could be case-dependent. Moreover, the implementation of speed limits also plays an important role in route choice behaviors (Madireddy et al., 2011; Nitzsche and Tscharaktschiew, 2013). Yet, how the new distribution of vehicles across different routes affects the origin–destination (OD) travel time (i.e., the effect on traffic efficiency at a more macroscopic level) is also still unclear. In terms of environmental externalities, here we refer to fuel consumption, exhaust emissions, and traffic noise. Intuitively, one can expect reductions in these figures in low-speed-limit situations considering that frequent accelerations/decelerations (the main contributor to the three figures) can be mitigated (Madireddy et al., 2011; Grumert et al., 2015). However, if traffic efficiency is significantly undermined by speed limit reduction, it is possible that the delay increase counteracts the benefits gained.

Considering the ambiguous impact of speed limits on the three aforementioned aspects, this paper aims to propose a practical simulation-based framework to assess the potential implications of speed limit policies systemically. In particular, the policy will be evaluated from the perspective of road safety, traffic efficiency, and environmental externalities. To this end, multiple key performance indicators (KPIs) are modeled and embedded to quantify the impacts at different aggregation levels (i.e., link level, route level, OD level, and network level), striving for a complete measurement. Such a framework can be used as an economical evidence collection method for an evidence-based policymaking approach to speed limit policies. Furthermore, to validate the present framework, a case study is conducted in a residential area within the city center of Munich, Germany. Numerous scenarios with different speed limit regulations and driver compliance levels are designed and compared. It is worth mentioning that, the impact of speed limits on an urban residential area is also a scope left for exploration in the existing literature.

The remainder of the paper is structured as follows. Section 2 summarizes the related literature. In Section 3, the evaluation framework for speed limit policies is presented. In Section 4, methods for measuring road safety, traffic efficiency, and environmental impacts are introduced sequentially. Section 5 describes the experimental design in detail, including the introduction to the study area, experiment scenarios design, and calibration procedure. In Section 6, the experiment results are systematically analyzed at different levels and angles. Section 7 discusses the limitations of this paper and future works. Finally, conclusions are drawn in Section 8.

2. Related literature

This section reviews the literature on (1) the implications of speed limits on road safety, traffic efficiency, and the environment, (2) the area-wise influence of speed limits, particularly on urban residential areas, and (3) speed limit policy evaluation via simulation.

2.1. Effects on road safety, traffic efficiency, and the environment

Many studies have been conducted to quantitatively evaluate the effects of speed limit implementation from different perspectives (namely, road safety, traffic efficiency, and the environment). Some mainly focused on one of the three aspects. For example, Makarewicz and Kokowski (2007) and Lan and Cai (2021) studied the impact of speed control on road traffic noise and uncovered the significance of traffic speed in the prediction of traffic noise emission. Renski et al. (1999) and De Pauw et al. (2014) tried to model the relationship between speed limit and crash rate, as well as the number of crashes resulting in serious injuries and fatalities. They found that speed limit reduction is beneficial to improving traffic crash numbers. Similarly, Amador and Willis (2014) pointed out that road safety practices associated with the enforcement of speed limits are one of the most significant measures pertaining to the reduction of fatalities, injury rates, and property damage accidents. Besides, Lu et al. (2011) combined VSL and coordinated ramp metering (CRM) to formulate a control strategy to mitigate the impairment of bottleneck flow on traffic efficiency (travel time delay). Considering the possibility of bottleneck formation at sag curves due to driving behavior changes, Nezafat et al. (2018) applied a simulation-based feedback control algorithm to optimize the speed limits imposed on connected vehicles (CVs) to maximize the traffic throughput.

Further, some have taken into account the broader effect of speed limits from multiple aspects in analyses. Most of them are dedicated to developing effective VSL control algorithms and evaluating the effectiveness of the combined model that integrates other control components. Also focusing on bottleneck flow, Jo et al. (2012) was proposed to improve the safety and travel delay situation under congested traffic scenarios on urban freeways by utilizing a variable speed limit (VSL) control algorithm driven by loop data. The classic trade-off between safety benefits and delay in travel time has also been accounted for in other speed limit strategy optimization problems like You et al. (2018) and economic evaluation models like Hensher (2006). Grumert et al. (2015) incorporated VSL with infrastructure to vehicles (I2V) communication technique and autonomous vehicles (AVs) to explore the potential benefits of cooperative individualized speed limits to traffic efficiency and the environment. Likewise, Sadat and Celikoglu (2017), Di Costanzo et al. (2020) and Tscharaktschiew (2020) also attempted to evaluate speed limits with an objective function comprising both safety and environmental impacts. A simulation-based evaluation was carried on in the first two studies, while a site data-based analysis and an economic equilibrium model were adopted in the third and the last, respectively. Furthermore, in Zhang and Ioannou (2016), VSL was combined with a lane change controller (LCC) to fix the inconsistency issue of travel time improvement observed in micro- and macro-scopic models using VSL alone. The combined control strategy also rendered consistent results in safety and environmental impact. The complete effect of speed limits has also been considered in Soriguera et al. (2013) and van Benthem (2015). They pointed out that the benefits of speed limit implementation depend on the relation between the value of traffic externalities and the marginal cost of travel times, and evaluating speed limits from a single aspect may lead to incorrect conclusions.

However, VSL is difficult to implement and requires a specific control algorithm to tune the value according to the prediction results of traffic speed and volume. The effectiveness of VSL is thus also highly dependent on the accuracy of the embedded prediction component. On the contrary, the (fixed) speed limit policy is easy to implement and requires not more than a speed limit sign, which generally can also attain acceptable results. In particular to area-wise implementations, the simply fixed speed limit will also not create confusion for the local residents like VSL. Moreover, we note that the works mentioned above are either focused on urban motorways or freeways/highways/interstates. It follows that most speed limit evaluations in the existing literature are limited to the link level. Few studies have investigated the impact of speed limits on urban residential areas from multiple levels.

2.2. Influence on urban residential areas

Madireddy et al. (2011) performed a before–after exhaust emissions analysis for the speed limit strategy in an urban residential area (Zurenborg) in Antwerp, Belgium. The simulation results showed that as the speed limit reducing from 50 km/h to 30 km/h, the emissions of CO_2 and NO_x declined over 26%, and vehicle kilometers traveled (VKT) within the study area felled by 14% due to vehicle rerouting. However, it overlooked the difference in safety and efficiency. Conversely, Islam and El-Basyouny (2015) applied a full Bayesian before–after evaluation method to measure the safety effects of reducing posted speed limit for eight urban residential areas located in the city of Edmonton in Alberta, Canada, while efficiency and environmental impact were neglected. Based on an online survey and speed measurements at more than 70 road sites in a residential area in Melbourne, Australia, Fildes et al. (2019) concluded that lower speed limits would improve the safety and attractiveness of the region, and can receive good community support. As claimed by Slavik and Gnap (2020), housing is the main function of residential areas that should have priority over others. It means that residents indeed would probably support reducing speed limits and installing speed-limiting devices within residential areas to alleviate noise and exhaust emissions. Differently, Nitzsche and Tscharaktschiew (2013) proposed a spatial computable general equilibrium model (CGE) to measure the area-wise effect of speed limits from an economic perspective, where all metrics were translated into monetary amounts for comparison purposes. While it is a comprehensive assessment framework that even considers influential factors apart from transportation, it can only provide a rough estimation and is less accurate than microscopic traffic simulations.

2.3. Simulation-based speed limit evaluation

Simulation models can generate detailed operation data of vehicles, such as instantaneous speed, acceleration, and emissions, and therefore have been widely employed in the literature. The simulation data can be used to model and calculate the metrics and indicators for measuring road safety, traffic efficiency, and environmental impacts. Accordingly, it has become an economical alternative to collecting evidence for evidence-based policymaking. For ease of reading, Table 1 lists some selected publications and compares their experimental setups, including the implications considered, study area, the method used, VSL usage, and the cooperation with other controllers. The publications are ordered based on “Study area” and the year of publication. From the table, we can see that the literature efforts that conduct speed limit policy investigations employ either of the three methods between site data analyses, economic equilibrium models, and simulation-based approaches. However, most studies focused on the effect at the link level, e.g., highways and freeways. Few have measured the area-wise effect of speed limits, i.e., network-level evaluation. More importantly, none have systematically investigated the complete effect of speed limits on urban residential areas using microscopic simulation models. It is worth mentioning that, microscopic models allow data aggregation into multiple spatio-temporal granularity levels so as to provide a thorough comparison between different policy scenarios.

Table 1
Experimental setups of selected literature.

Paper	Safety	Efficiency	Environment	Study area	Model	VSL	Others
Makarewicz and Kokowski (2007)	No	No	Yes	General roads	Site data	No	No
Amador and Willis (2014)	Yes	No	No	General roads	Site data	No	No
Grumert et al. (2015)	No	Yes	Yes	Motorways	Simulation	Yes	V2I, AV
Farrag et al. (2020)	Yes	Yes	Yes	Expressways	Simulation	Yes	CV
Renski et al. (1999)	Yes	No	No	Highways	Site data	No	No
De Pauw et al. (2014)	Yes	No	No	Highways	Site data	No	No
Tscharaktschiew (2020)	No	Yes	Yes	Highways	Equilibrium	No	No
Hensher (2006)	Yes	Yes	No	Freeways	Site data	No	No
Lu et al. (2011)	No	Yes	No	Freeways	Simulation	Yes	CRM
Jo et al. (2012)	Yes	Yes	No	Freeways	Simulation	Yes	No
Soriguera et al. (2013)	Yes	Yes	Yes	Freeways	Simulation	Yes	No
van Benthem (2015)	Yes	Yes	Yes	Freeways	Site data	No	No
Zhang and Ioannou (2016)	Yes	Yes	Yes	Freeways	Simulation	Yes	LCC
Sadat and Celikoglu (2017)	No	Yes	Yes	Freeways	Simulation	Yes	No
Nezafat et al. (2018)	No	Yes	No	Freeways	Simulation	Yes	CV
You et al. (2018)	Yes	Yes	No	Freeways	Simulation	Yes	No
Di Costanzo et al. (2020)	No	Yes	Yes	Freeways	Simulation	Yes	No
Nitzsche and Tscharaktschiew (2013)	Yes	Yes	Yes	Urban areas	Equilibrium	No	No
Lan and Cai (2021)	No	No	Yes	Urban areas	Site data	No	No
Madireddy et al. (2011)	No	No	Yes	Residential areas	Simulation	No	No
Islam and El-Basyouny (2015)	Yes	No	No	Residential areas	Site data	No	No
Fildes et al. (2019)	Yes	No	No	Residential areas	Site data	No	No
Slavik and Gnap (2020)	No	Yes	Yes	Residential areas	Site data	No	No

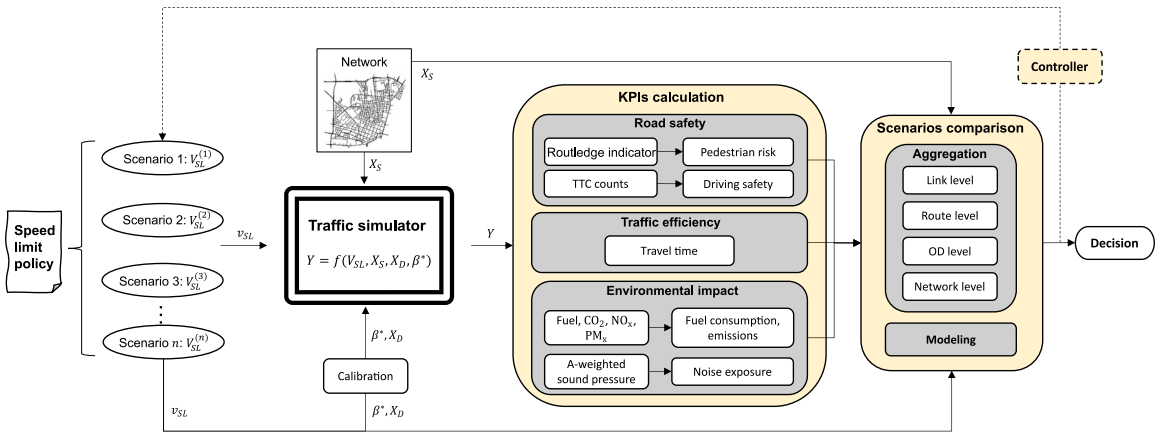

Fig. 1. Simulation-based policy evaluation framework.

3. Simulation-based policy evaluation framework

Since simulation-based approaches are generally more economical than site data collection and more accurate than economic equilibrium models, this study proposes a simulation-based policy evaluation framework that comprehensively evaluates the effect of different speed limits for urban residential areas (Fig. 1). The systematic evaluation framework leverages microscopic traffic models for evaluating speed limit policies with respect to their impact on road safety, traffic efficiency, and the environment at different aggregation levels. Therefore, the three prominent aspects of the framework include, (1) traffic modeling, (2) key performance indicators (KPIs) modeling, and (3) policy scenario evaluation. Note that while the developed framework is utilized in the current study to evaluate speed limit policies, it also acts as a template to establish other similar evidence-based policies.

The first component consists of the microscopic traffic simulator of the urban network that models detailed vehicle driving behaviors with dynamic route choices. For the sake of simulation reliability, both the OD demand matrix (X_D) and simulator embedded models (β^*) (car-following model, lane-changing model, route choice model, traffic light system, etc.) require rigorous calibrations using suitable demand and supply estimation algorithm (discussed in Section 5.3). The traffic simulator, configured with policy scenario (V_{SL}), case network system (X_S) and demand patterns, is used to simulate the traffic for each scenario. The second component utilizes the fine-grained traffic-related outputs (Y) (traffic volume, vehicle speed, acceleration rate, etc.) generated by the microscopic simulation to calculate the policy performance indicators or KPIs. These KPIs are proposed from the perspective of road safety, traffic efficiency, and environmental impact. Modeling all three aspects allows us to articulate the actual policy impact

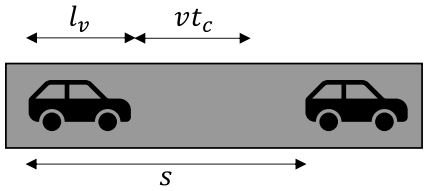

Fig. 2. Routledge indicator.

better and provide opportunities to balance policy-related benefits and costs. This component is discussed in more detail under Section 4.

Finally, the third component defines and evaluates different policy scenarios. Scenario definition in the case of speed limit policies covers defining different speed levels for corresponding road types in the urban network. Whereas, the scenario evaluation part combines and interprets the KPIs at different aggregation levels, which provides a wider interpretability toward the possible policy implications. Instead of investigating the effect merely at the link level, we consider the KPIs at the link level, route level, OD level, and network level. Different simulated scenarios are later compared at each level. Note that the component can also be further extended to model the relationships between different inputs (e.g., scenario-related variables, parameters from supply and demand) and the value of interest, e.g., the spatial difference of the influence on traffic efficiency (demonstrated in Section 7.1 using regression analysis). Such a model can assist in understanding the sensitivity of the given KPI against individual model parameters and allows effective designing of new scenarios, especially when all initial scenarios cannot satisfy the requirements. Similarly, the aggregated values can be all converted into monetary costs as in Nitzsche and Tscharaktschiew (2013) for modeling purposes for understanding the relationship between the inputs and the complete effect. Finally, given a predefined objective (e.g., most improvement in pedestrian safety), the comparison evaluations are examined and the most effective scenario is chosen to support the speed limit policymaking.

Theoretically, an additional controller component (dashed box) can be integrated into the proposed framework to dynamically supervise the design of scenarios via a feedback connection from the scenario comparison component to the scenarios design component (with the controller in-between), especially in the connected and autonomous vehicles (CAVs) era where vehicles respect the rules strictly. This, actually, provides an approach to develop a network-wide VSL system based on the synthesized effect on the residential area. Yet, this may be inapplicable in the foreseeable future when human-driven vehicles are still the major participant in traffic considering that human drivers have difficulty in capturing the real-time changes in speed limits. But, it is out of the scope of this paper and is not discussed here.

4. Modeling key performance indicators (KPIs)

This section elaborates on the KPIs for road safety, traffic efficiency and environmental impacts considered in this study subsequently.

4.1. Road safety

4.1.1. Accident risk exposure for pedestrians

Several indicators and methods have been developed to measure the accident risk of crossing for pedestrians. Here we apply a modified version of the indicator proposed by Routledge et al. (1974a,b) for this purpose. The original indicator (named Routledge indicator hereafter) was first conceptualized to enable the method for measuring the accidents per road crossing presented in Howarth et al. (1974) to forecast the risk of crossing the given road. However, it cannot precisely reflect the situation in dense traffic conditions. As a result, Lassarre et al. (2007) constructs a modified version to overcome this drawback and adapt it to the multi-lane road context.

The Routledge indicator measures the probability of a pedestrian being hit by a vehicle under a certain traffic density situation if he/she crosses the road randomly and both the pedestrian and the vehicle take no evasive action (both are heedless). It is given by

$$r_c = \frac{l_v + vt_c}{s} \tag{1}$$

where l_v and v are the average length and speed of vehicles respectively, t_c denotes the time needed for pedestrians to cross the road, and s is the space headway between every two vehicles. It measures the proportion of road 'occupied' by the traffic as shown in Fig. 2. A larger value of r_c means there is less space available for pedestrians to cross the road and thus is more dangerous.

Assuming a linear relationship exists between traffic density and speed (Greenshields et al., 1935), one can calculate the risk exposure under different traffic speeds based on prior knowledge (about free-flow speed v_f, length of vehicles l_v, and crossing time t_c) by

$$r_c = (1 - \frac{v}{v_f})(1 + \frac{vt_c}{l_v}) \tag{2}$$

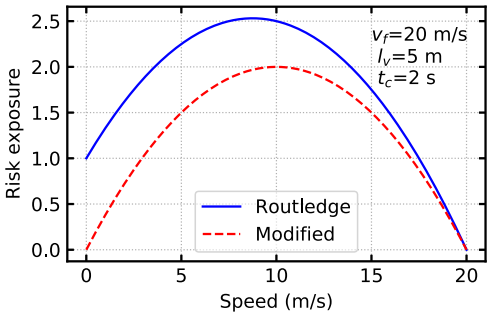

Fig. 3. Comparison of the Routledge indicator and its modified.
Source: Adapted from Lassarre et al. (2007).

Fig. 3 depicts the exposure line under $v_f = 20$ m/s, $l_v = 5$ m, and $t_c = 2$ s. Considering when the traffic speed $v = 0$ (i.e., in saturation conditions), the accident risk is relatively low, though it has limited accessibility for crossing. Obviously, the Routledge indicator is not representative in nearly saturated situations like this. As such, Lassarre et al. (2007) enhanced it by suppressing the term related to the saturation density as Eq. (3).

$$r'_c = (1 - \frac{v}{v_f})\frac{vt_c}{l_v} = k_j(1 - \frac{v}{v_f})vt_c = t_c q \tag{3}$$

where k_j is the jam density; q is the traffic volume. For a road with n_l lanes, assuming the traffic is evenly distributed, the equation becomes

$$r'_c(n_l) = \frac{t_c q}{n_l}\sum_{i=1}^{n_l} i \tag{4}$$

Fig. 3 also shows the line of the modified Routledge indicator, which has become a symmetric parabola. This modified Routledge indicator is used to evaluate the crossing risk for pedestrians in this study. Going forward, the modified Routledge indicator will be referred to as the Routledge indicator.

4.1.2. Driving safety of vehicles

As the group being affected directly by the speed limit policy, the driving safety of vehicles is also involved in the evaluation of road safety. Time-to-collision, which is one of the most popular indicators for assessing driving risk, is used for this purpose. It measures the time needed for a follower to crash into its leader if the relative speed stays unchanged, and is given by

$$TTC = \begin{cases} \frac{x_l - x_o - l_o}{v_o - v_l} & \text{if } v_o > v_l \\ \infty & \text{otherwise} \end{cases} \tag{5}$$

where x_l, x_o denote the longitudinal location of the leader and the follower respectively, while v_l and v_o indicate the respective speed. l_o is the length of the following vehicle. Following the recommendation by Papadoulis et al. (2019) and Zhang et al. (2020), we record a situation as dangerous when TTC is not greater than 2 s. The count of records is then used to evaluate the driving safety situation.

4.2. Traffic efficiency

Travel time is utilized as the metric to measure traffic efficiency under different speed limit scenarios. Understanding the influence of speed limit on traffic efficiency is not straightforward, because it is the result of an equilibrium formed from several conflict effects. These conflicts can unilaterally determine the final performance and thus need to be considered explicitly. Modeling and estimating these conflicts is one reason to use the microscopic traffic simulator.

Fig. 4 illustrates the effect flow of implementing speed limit reduction on some links. Reducing the speed limit can harmonize the traffic on target links during congested periods, but also slows down vehicles in free flow and median flow situations. The state changes on these links will affect the route choices of vehicles and further change the traffic distribution across the network. The traffic assignment finally acts on the traffic efficiency of the whole network represented by the disparities in travel time before and after implementing the policy. On the other hand, the updated traffic assignment also urges practitioners/engineers to optimize the traffic lights system accordingly to improve the network capacity. However, it takes time for a network to reach a new steady state. The route choice behavior of a driver is dependent on the latest information on routes, such as travel time and traffic light configurations (coordination and adaptation), and experience. In other words, the traffic distribution across the network continues altering until the new equilibrium has been established between network supply and route choice.

Interestingly, this effect flow is similar to the calculation procedure of the dynamic user equilibrium (DUE) (Wardrop, 1952) via an iterative simulation-based route choice algorithm. But this effect flow reflects the process between equilibrium states under two

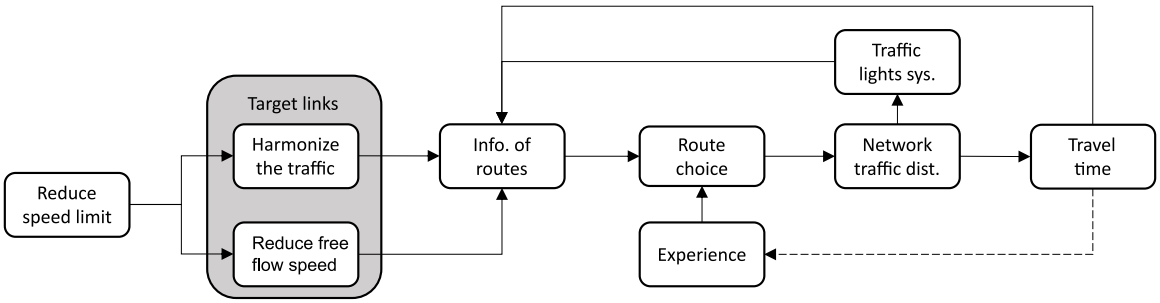

Fig. 4. The influence of the speed limit reduction.

speed limit scenarios, while the iterative simulation-based traffic assignment is for distributing routes to vehicles that could produce a user equilibrium. Ideally, the comparison of different policy scenarios should be conducted under respective user equilibrium states. Note, the iterative simulation-based traffic assignment is used to compute the user equilibrium state for each. However, in reality, a proportion of people (e.g., non-routine drivers) conform to the assumption of dynamic stochastic assignment in regard to route choice behavior (i.e., continuously using the navigation to get dynamic user optimum under a given stochastic state of the network). As a result, simulations should be conducted with imperfect DUE assignment, or more specifically, with a combination of DUE and dynamic stochastic user assignment. This is portrayed in Section 5.2.

4.3. Environmental impacts

4.3.1. Fuel consumption and exhaust emissions

Transportation is one of the main contributors to energy consumption, climate change and air pollution (Zhao et al., 2013), which are in correspondence with fuel consumption, CO_2 emission and pollutant emissions (e.g., NO_x, PM_x), respectively. Hence, it is sensible to evaluate the environmental impacts of transportation policies before they are in force. A microscopic traffic simulator equipped with a calibrated emission model is useful in predicting the performance of such policies (Krajzewicz et al., 2015). In this study, the HBEFA derivation (version 3.1) (Infras, 2010) embedded in SUMO is used to estimate vehicular pollutant emission. HBEFA was developed using the basic emission factors provided by the well-known PHEM model (a de facto European reference) (Krajzewicz et al., 2015). PHEM computes the engine power and engine speed based on the vehicle speed, road gradient, driving resistances and losses in the transmission system. The engine power and speed are then used for the calculation of fuel consumption and exhaust emissions. However, the computation complexity impedes the application of PHEM to large-scale scenarios. Thus, HBEFA simplifies the calculation of the engine power needed to overcome the driving resistance force as a continuous function, which is given by

$$\mathrm{m}_E = c_0 + c_1 v a + c_2 v a^2 + c_3 v + c_4 v^2 + c_5 v^3 \tag{6}$$

where m_E is the amount of emission type E, v the instantaneous speed of vehicle, a the instantaneous acceleration rate. For a specific vehicle class (emission class), the coefficients set $c_i(\forall i \in [1,2,3,4,5])$ are estimated by fitting with the corresponding vehicle data extracted from the HBEFA database via linear regression. For instance, the coefficients for the gasoline-powered Euro 4 passenger car model are calibrated with the emission data of 208 typical vehicles. This approach applies to fuel consumption and all emission types. In other words, they shared the same functional form but with different coefficient setups. Therefore, at each simulation step, given the velocity and acceleration of vehicles, fuel consumption and emissions can be derived.

4.3.2. Noise exposure

People living in residential areas with heavy traffic are susceptible to the noise produced by vehicles. As such, traffic noise has become an important consideration of the environmental impact. We apply the Harmonoise model (Nota et al., 2005) to estimate the traffic noise. The Harmonoise model calculates the equivalent A-weighted sound pressure levels caused by traffic taking into account both the sound power outputted from noise sources and the attenuation during the propagation.

Fig. 5 shows the simplified schematic graph of this model. In the noise sources modeling, a source line, which consists of a set of incoherent point sources (point sources are discretized as line segments), is defined based on the vehicle model and the traffic model. The vehicle model is used to measure the sound power of a single moving vehicle, wherein three subsources at 0.01 m, 0.30 m and 0.75 m (only for heavy vehicles) above the road surface are explicitly modeled. Mathematically, for a vehicle category z and a 1/3 octave band k, the strength of a subsource s is calculated as

$$L_{W,s,z,k} = L_{WR,s,z,k} \oplus L_{WT,s,z,k} \tag{7}$$

$$L_{WR,s,z,k} = \alpha_{R,z,k} + \beta_{R,z,k} \lg\left(\frac{v}{v_{ref}}\right) + 10\lg(0.8) + C_{dir,s,k} + C_{surf,z,k} + C_{region,z,k} \tag{8}$$

$$L_{WT,s,z,k} = \alpha_{T,z,k} + \beta_{T,z,k} \lg\left(\frac{v - v_{ref}}{v_{ref}}\right) + 10\lg(0.2) + C_{dir,s,k} + C_{dc,z} \tag{9}$$

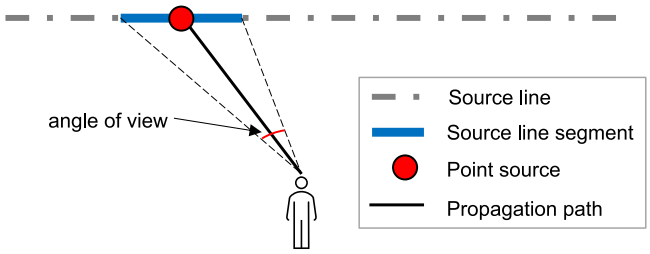

Fig. 5. Noise sources and noise propagation.
Source: Adapted from Nota et al. (2005).

where L_W is the sound power, L_{WR} and L_{WT} are the rolling and traction noise sound powers, respectively. α_R and β_R are rolling noise coefficients. α_T and β_T are rolling noise coefficients. v is the vehicle speed, v_{ref} is the reference speed. $C_{dir}, C_{surf}, C_{region}$ and C_{dc} are the correction factors for source directivity, road surface, deviation in the sound power output of the regional vehicle fleet, and driving conditions, respectively. We refer the interested reader to Nota et al. (2005) for more details of these variables and coefficient values for different vehicle classes.

The traffic model, on the other hand, combines the outputs from numerous vehicles into the sound power per unit of the source line, which can be regarded as a statistical description of vehicle models.

$$L'_{W,z,k} = L_{W,z,k} + 10\lg\left(\frac{Q_z v_{ref}}{1000 Q_{ref} v_{eq,z}}\right) \tag{10}$$

$$L'_{W,k} = 10\lg \sum_z 10^{0.1 L'_{W,z,k}} \tag{11}$$

where $v_{eq,k}$ is the equivalent vehicle speed of category k, v_{ref} is the reference vehicle speed, Q_k is the traffic flow of category k, and Q_{ref} is the reference traffic flow.

In propagation modeling, various factors could strengthen or weaken the acoustical energy, such as geometrical divergence, and atmospheric absorption. The equivalent sound pressure level for a specific receiver is the aggregated result of several propagation paths.

5. Experimental design

5.1. Study area and simulation setup

Maxvorstadt and Schwabing, located in the city center of Munich, is a residential area in the area surrounded by the inner ring of Munich (i.e., Bundesstrasse 2R). We implement the case study in this area to validate the proposed simulation-based evaluation framework for speed limit policies. Fig. 6(a) shows the map of the study area along with the delineation of traffic analysis zones (TAZs). This 5 km × 5 km area is divided into 16 TAZs together with 8 external zones around. Fig. 6(b) gives the network structure and indicates the road type of all links with different colors, from residential links to urban motorways. The locations of the 11 detectors for traffic measurements are also indicated in the figure. We simulate the traffic between 5 am and 10 am, considering the first and last hour as the warm-up and dissipation periods, respectively. The calibration process of traffic demand and the models assembled into the simulator (driving behavior models, etc.) are discussed in Section 5.3.

5.2. Experiment design

Three speed limit scenarios listed in Table 2 are designed. The speed limits of motorways (pedestrian crossing is not allowed) and residential links are kept constant in all scenarios. The Base scenario conforms to the real speed limit setup, where the speed limits for primary, secondary and tertiary links are 60 km/h, 50 km/h and 40 km/h, respectively. The speed limits of these links are set to 40 km/h and 30 km/h, respectively, in the other two scenarios, i.e., SL40 and SL30. The experimental design is partially inspired by Nitzsche and Tscharaktschiew (2013), which found that planning a *slow zone* can enhance social welfare and is deemed to be a promising speed limit policy. By the speed limit scenarios devised in this paper, we attempt to make the study area a slow zone. Identical speed limits also add homogeneity in network information and facilitate ease in network perception and interactions for all road users.

Considering their convenience and efficiency, microscopic traffic simulators have been extensively applied to estimate traffic and evaluate traffic control and management policies. SUMO (Lopez et al., 2018) is used for both the calibration task and experiment implementation in this study. Note that for each scenario, final results are derived by averaging outputs of 10 simulation replications with different random seeds to cater to the model stochasticity (vehicle arrivals, route choice, etc.). The set of random seeds is kept constant among different scenarios, which helps avoid stochastic variations among simulations. More importantly, this allows analyzing the effect of reducing speed limits on the route choices of vehicles. All simulations are modeled at the microscopic

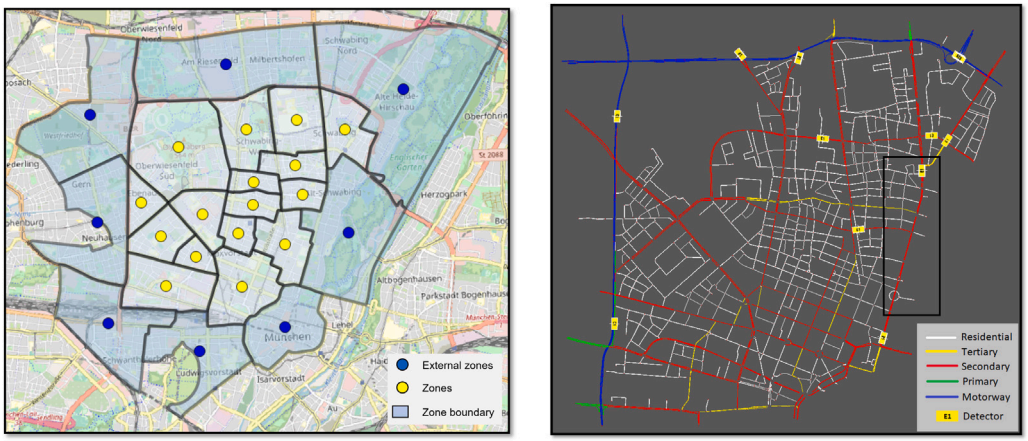

(a) Traffic zones (b) Network and road types

Fig. 6. The study area. (For interpretation of the references to color in this figure legend, the reader is referred to the web version of this article.)

Table 2
Scenario design.

Scenarios	Motorway	Primary	Secondary	Tertiary	Residential
Base	80 km/h	60 km/h	50 km/h	40 km/h	30 km/h
SL40	80 km/h	40 km/h	40 km/h	40 km/h	30 km/h
SL30	80 km/h	30 km/h	30 km/h	30 km/h	30 km/h

resolution with a 0.1 s step length. A fine simulation step can avoid unexpected processing errors and can also improve the accuracy of the computation of fuel consumption, exhaust emissions, traffic noise, and the counting of TTC critical moments. Traffic assignment is carried via the non-iterative dynamic stochastic user assignment method (i.e., automated routing in SUMO). As a variant of dynamic user assignment, it assigns the respective fastest routes to vehicles based on their departure time. Note, edge costs (here, travel time) for route cost calculation are periodically updated. This traffic assignment method can be used to approximate the DUE with much fewer computation costs if the updating interval is small enough and the proportion of vehicles with rerouting capability increases (Ashfaq et al., 2021). However, as mentioned in Section 4.2, in reality, traffic assignment is a combination of DUE and dynamic stochastic user assignment due to the existence of non-routine drivers in addition to commuters. Thus, the proportion of vehicles with rerouting capacity should be limited to capture the dynamic stochastic part. This proportion is regarded as the drivers who refer to routing navigation devices for real-time network information during the trip. In addition, as traffic will be redistributed in different scenarios, the traffic light system should be optimized correspondingly to guarantee the comparison and analysis are conducted under the optimal operating state of each scenario. Therefore, the traffic light coordination and adaptation are respectively optimized for different scenarios with the tools[1] recommended by SUMO.

5.3. Network calibration

Among the modeling steps, model calibration is significantly important to recurrent realistic traffic flows. For the sake of reliability, model calibration should be conducted on both supply and demand sides. In this study, the supply model is calibrated by estimating the driving behavioral parameters. The Wiedemann-99 model is used for modeling car-following behavior. The model parameters are calibrated using the Simultaneous Perturbation Stochastic Approximation (SPSA) algorithm (Spall, 1998), fitting upon the data collected at the corridor (a secondary road from Leopoldstrasse to Ludwigstrasse, about 2.5 km long) marked in Fig. 6(b) for the period between 17:00 and 18:00. Though a car-following model calibrated with the data collected from a secondary road may be biased to the traffic at residential links and motorways, the four regimes defined in Wiedemann-99 for distinguishing the interaction of vehicles in different traffic states can somehow mitigate the influence (Wiedemann and Reiter, 1992). Wiedemann-99 has also been widely used in microscopic traffic simulation for both lane-based and non-lane-based conditions (Anil Chaudhari et al., 2022). Besides, as one of the busiest corridors in Munich, that road segment, on the one hand, can often observe frequent interactions between vehicles and pedestrians as in the residential links. On the other hand, it is also partially controlled as those motorways. Therefore, the calibrated Wiedemann-99 model should be capable of representing the traffic characteristics within this study area. Using the maneuver data measured at the same site to calibrate the driving behaviors also further strengthens the reliability of simulation results. We refer the interested reader to Dinar (2020) for more details about the dataset. Table 3 shows the

[1] See https://sumo.dlr.de/docs/Tools/tls.html for more information about these tools.

Table 3
Calibrated values of the Wiedemann-99 model.

Variable	Value	Variable	Value
CC0 [m]	1.50	CC5 [m/s]	0.35
CC1 [s]	1.50	CC6 [10^{-4} rad/s]	11.44
CC2 [m]	4.00	CC7 [m/s^2]	0.25
CC3 [s]	−8.00	CC8 [m/s^2]	4.00
CC4 [m/s]	−0.40	CC9 [m/s^2]	1.50

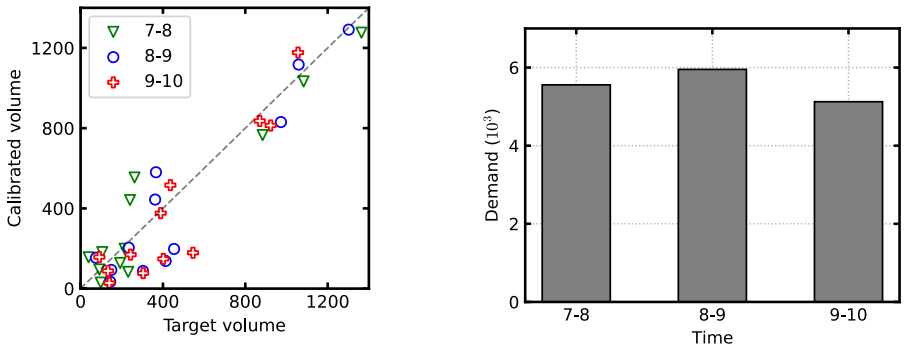

(a) Calibrated traffic vs. observed traffic (b) Calibrated demand

Fig. 7. Calibration results.

calibration result of the Wiedemann-99 car-following model. The calibrated model is integrated into SUMO for running the following experiments. Regarding lane-changing behavior, a four-layer control architecture with distinct motivations for lane change at each layer (i.e., strategic, cooperative, tactical, and regulatory motivations) is applied in SUMO. At each simulation step, it determines the vehicle's decision on lane-changing based on the current and historical surrounding traffic conditions and adjusts the velocity appropriately to ensure the successful execution of the decision. We applied the parameters from Erdmann (2015) in the following experiments.

On the other hand, the demand side is represented by the OD matrix, which contains the demand information of all TAZ OD pairs. Note, the study area only represents a portion of the Munich city center, and only a section of the Munich inner ring is included. Consequently, the amount of through traffic will increase dramatically in simulations due to: (1) All trips from/to external zones can only use the network provided in Fig. 6(b) to reach their destinations, which is inconsistent with reality in which some are carried by the paths outside this network (e.g., the entire Munich network); (2) Aggregating the TAZs around the study area to create external zones has destroyed the demand structure of the OD matrix, which requires amendments in the calibration process. To address this issue, we first apply the SPSA algorithm to correct the traffic demand from/to external zones. Utilizing the corrected OD matrix as the prior, we then employ the PC-SPSA algorithm (Qurashi et al., 2022) to calibrate the whole OD matrix. Traffic measurements (here, traffic counts) are aggregated into a one-hour interval for each detector. The Root Mean Square Normalized (RMSN) error between the observed traffic counts and the simulated traffic counts is used to measure the goodness-of-fit, which is given by

$$RMSN = \frac{\sqrt{N \sum_{i=1}^{N} (\hat{y}_i - y_i)^2}}{\sum_{i=1}^{N} y_i} \tag{12}$$

where N is the number of detectors, y_i and $\hat{y}_i$ are the observed and simulated traffic counts at detector i. We note that demand patterns between consecutive time intervals should not be very different. To mitigate the noise introduced by the calibration algorithm to the demand pattern, the OD matrices of the considered intervals are corrected simultaneously at the step of the SPSA application. Fig. 7(a) compares the calibrated traffic counts and the observed traffic counts using a 45-degree plot. Clearly, traffic counts are fitted well, especially at busy links where the impact of traffic is more concerning. Fig. 7(b) gives the total demand within each time interval after calibration.

6. Results analysis

In this section, the effects of speed limits are assessed at four different levels. For calculating the Routledge indicator, we assume the average crossing speed is 1.31 m/s as recommended by Onelcin and Alver (2017). Since the lane width in SUMO is 3.2 m, then the time needed for a pedestrian to cross a lane is $t_c = 2.44$ s. Trucks are not allowed in the simulation as the study focuses on the residential network. Assume all vehicles have the size 5 m (length) × 1.8 m (width) × 1.5 m (height). Besides, the HBEFA emission

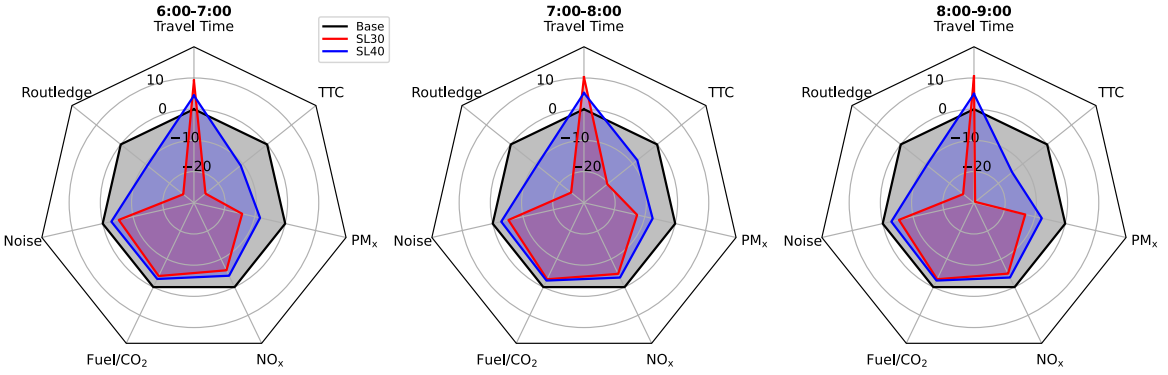

Fig. 8. Network-wide metrics comparison.

model and Harmonoise model have been embedded in SUMO so that we can obtain relevant data from the simulation directly. For the HBEFA model, a gasoline-powered Euro 4 passenger car model is used.

First, by comparing the KPIs under different scenarios at the network level, we start with an overall understanding of the impact of speed limits on the concerned aspects. Then, we pay attention to the changes at the link level to investigate how the effects distribute and aggregate, followed by the analysis of the influence on route choices. Finally, we analyze the changes in OD travel time.

6.1. Evaluation at the network level

Note that, the Routledge indicator and noise exposure are link-based metrics. For each scenario, the weighted average of the link-based metrics (weighted by the traffic volume of the link within the given hour) is used to measure its network-level performance. On the other hand, for other non-link-based metrics: The average travel time of all trips is compared; The TTC counts represent the sum of dangerous conflicts between vehicles; For the fuel consumption and exhaust emissions, the values are aggregated directly. Fig. 8 compares the performance of three scenarios on the KPIs. It shows the percentage change of different metrics in SL30 and SL40 compared to the Base scenario. In the HBEFA model, the CO_2 emission is proportional to the fuel consumption, so they are placed together in the chart. As can be seen, all values of the Base scenario are predefined as zero. The center value of the charts is −30%, and the outermost circle represents an increase of 20%. There is a 10% gap between every two circles. Clearly, SL30 and SL40 induce reductions in all metrics other than travel time. It means, reducing speed limits can enhance safety, including pedestrian safety and driving safety, and limit environmental externalities, including CO_2 emission, toxic exhausts, noise exposure and fuel consumption, within the residential area with the cost to traffic efficiency (i.e., travel time).

More specifically, in all time intervals, the crossing risk exposure in SL40 and SL30 reduce by more than 10% and 25%, respectively. The main trigger for this improvement is that more vehicles select the paths containing motorways when the speed limits of links within the residential area reduce. Driving safety has also improved, and the improvement is correlated to the traffic demand – a larger demand renders a slighter improvement. The speed limit is the most important factor as represented by the difference in the improvement between SL40 and SL30. The implementation of a stricter speed limit enforces some vehicles to change route choices and therefore alleviates the traffic congestion on busy links, which can, on the other hand, relieve the stop-and-go oscillations. This domino effect finally reduces the number of critical TTC moments. Moreover, both SL30 and SL40 lead to similar percentage changes in travel time, fuel consumption, noise exposure, and exhaust emissions, in all time intervals, while SL30 results in slightly larger improvements. Although a decision module is integrated into the proposed evaluation framework, no specific objective is proposed in this paper for the sake of generality. But, policymakers can adopt the framework to attain specific objectives. For example, if one places the same weight on all metrics, the smaller the area enclosed by the radar map is, the better the scenario. Clearly, SL30 is preferable in this case. Besides, analogous to the evaluation conducted in Nitzsche and Tscharaktschiew (2013), one can also translate the metrics into monetary costs such that different scenarios can be compared based on the urban economy.

Further, considering that not all drivers respect the speed limit regulation in reality, we conduct a sensitivity analysis on the compliance level of vehicles to the speed limits. Here the compliance level is evaluated from two aspects: (1) the percentage of vehicles that respect the speed limit; (2) the extent to which the desired driving speed of speedy vehicles exceeds the speed limit. A speed factor (SF) is defined for the latter aspect. Mathematically, $v_{desired} = SF \times SL$. The SF of speedy vehicles is assumed to follow a truncated normal distribution with a mean selected from $[1.1, 1.3, 1.5]$, a standard deviation of 0.1, and lie within $(0.5, 2)$. At the same time, the compliance percentage is selected from $[0.5, 0.6, 0.7, 0.8, 0.9]$. Note, the SF of normal vehicles will be all specified as 1. The sensitivity analysis experiments are conducted based on the SL40 scenario network setups for the interval 7 am–8 am. The performance of different compliance level scenarios in travel time, pedestrian risk exposure, vehicle crash risk, and CO_2 emission, are compared in Fig. 9. The results are extracted from 10 simulation replications. Clearly, the average travel time and vehicle crash risk are very sensitive to either compliance percentage or SF. To be specific, the average travel time increases with compliance

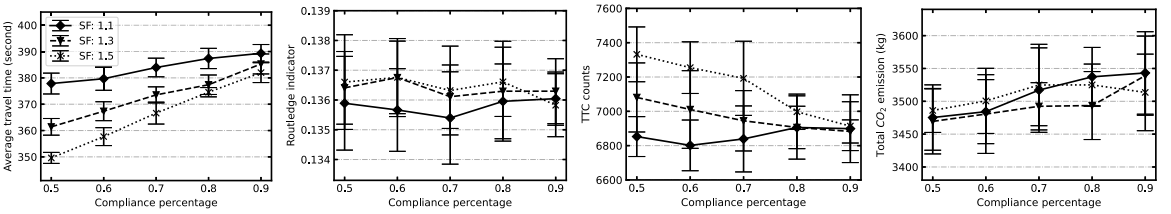

Fig. 9. Sensitivity analysis on compliance level of drivers to speed limits (based on SL40, 7 am–8 am).

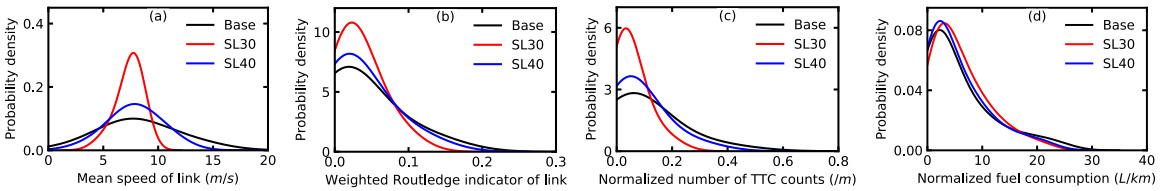

Fig. 10. Distribution of metrics at the link level (all links).

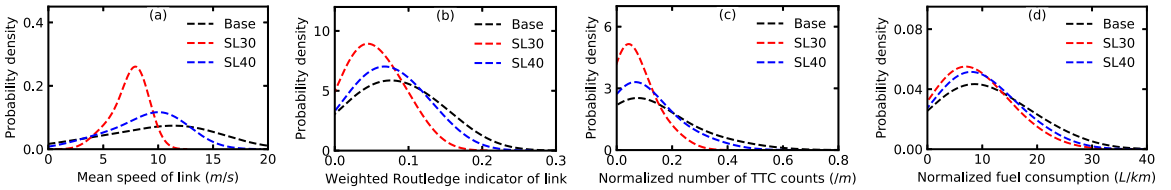

Fig. 11. Distribution of metrics at the link level (links with speed limit changed).

percentage and reduces with SF. Whereas, the count of critical TTC moments shows an opposite trend. Conversely, pedestrian risk exposure and CO_2 emission obtain similar values in these experiments. We clarify that in other experiments SF is assumed to follow a normal distribution, i.e., $SF \sim \mathcal{N}(1, 0.1)$, and is truncated in the interval $(0.2, 2)$.

6.2. Evaluation at the link level

Fig. 10 shows the distribution of the metrics for all links under different scenarios, while Fig. 11 presents that for the links with speed limit changed (target links). The metrics include the mean speed of vehicles, the weighted Routledge indicator (weighted by the traffic volume), the normalized number of critical TTC moments (normalized by the length of the link), and the normalized fuel consumption of traversing vehicles. At the link level, the mean speed of vehicles is a more plausible metric to describe traffic efficiency than average travel time, as the average travel time can be easily dominated by the length of the link. The distributions are approximated based on a Gaussian kernel.

As expected, the vehicle speed will accordingly decrease with the speed limit reduction, as shown in Fig. 10(a). Besides, the speed distribution becomes more and more concentrated from the Base scenario to SL40 to SL30. This, on the other hand, implies that the reduction of speed limits can contribute not only to the harmonization of traffic flow on the target links, but also to traffic flow over the network. Fig. 11(a) illustrates that, for the target links, the peaks of speed distributions are more distant. As the objects being affected directly, they observe a more obvious change in traffic state than the others. The decrease in speeds may harm traffic efficiency, but benefit safety at the same time. Regarding pedestrian risk exposure, Fig. 10(b) says that reducing speed limits can enhance pedestrian safety in most links, though the peak of distribution for the scenario with a stricter speed limit moves to the right. In contrast, for the target links, pedestrian safety can be improved and the peak also moves to the left in the scenario with a stricter speed limit. We can also observe a similar phenomenon in the distributions of fuel consumption from Figs. 10(d) and 11(d). The distributions of TTC counts have similar shapes in Figs. 10(c) and 11(c) indicating the effect on driving safety is similar for the target links and the whole network. Note, noise intensity is not dependent on the traffic volume and cannot be cumulatively calculated (the link with one vehicle passing and the link with one hundred vehicles passing may result in similar noise pressure levels), so it is not analyzed at the link level.

6.3. Influence on route choice

The area-wise effects of speed limit changes are achieved mainly by influencing the route choices of vehicles as explained in Section 4.2. Fig. 12 depicts the influence of speed limit on the travel time of trips, where the trips with routes changed compared

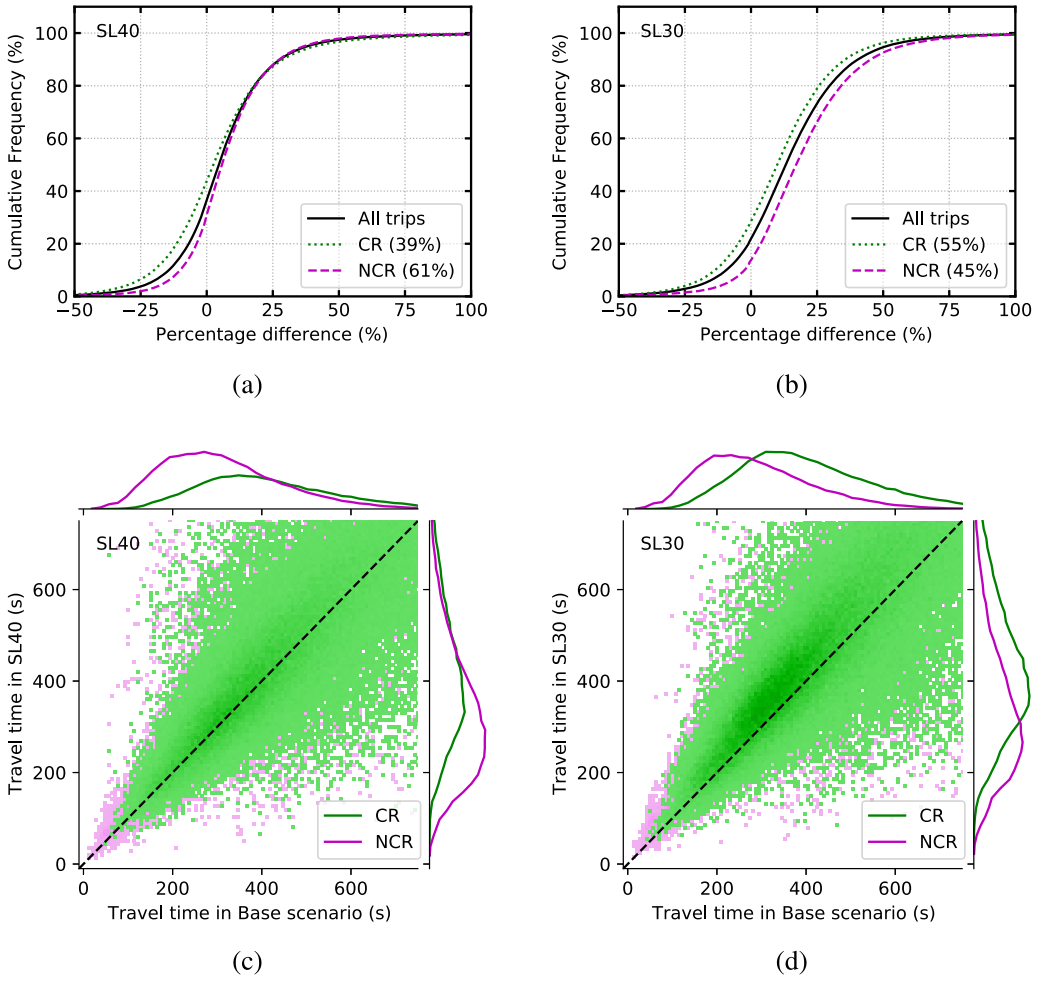

Fig. 12. The influence of speed limit on the trips travel time (CR: change routes; NCR: not change routes).

to the Base scenario and those that do not change are separately considered. For the sake of simplicity, we denote these two groups as CR and NCR, respectively.

The proportion of CR in SL40 is about 39%, and this number increases to 55% in SL30. By comparing the respective areas enclosed by the distribution curves of CR and NCR in Figs. 12(c) and 12(d), one can reach a similar conclusion, i.e., stricter speed limits cause more route changes. Moreover, all distributions for NCR skew to the right representing that short-distance (short-time) trips are less likely to change their routes. The potential reason is that short-distance trips have a lower probability of going through the links with speed limit changed. Hence, the influence on this group is weaker than another. The x-axis in Figs. 12(a) and 12(b) is the percentage difference of the travel time in the corresponding scenario compared to that in the Base scenario, and the y-axis is the cumulative probability. The distance between the cumulative distribution functions (CDFs) for CR and NCR in Figs. 12(a) and 12(b) at $x = 0$ reflects that the percentage of trips seeing an increase in travel time in NCR is more than that in CR. Specifically, it is about 10% more in SL40 and 15% more in SL30. Referring to the solid black curves in these two plots, the proportion of trips encountering an increase of more than 50% in travel time is very small (about 3% in SL40 and %7 in SL30). It means reducing speed limits will not extremely impede the travel of individuals. One may also notice that the CDF for CR and the CDF for NCR in SL40 are almost overlapped with each other when $x \geq 20$, while this phenomenon does not occur in SL30. It follows that, in SL40, the intensity of speed limit influence on CR and NCR are similar in the part of trips experiencing an increase of more than 20% in travel time. On the contrary, the influence intensity on CR and NCR keeps different in SL30. Furthermore, obviously, more trips are obstructed in SL30 than in SL40, as illustrated by the scatters dispersion from the diagonal dashed line in Figs. 12(d) and 12(c). Precisely, about 80% and 65% of trips are hindered in SL30 and SL40 respectively (which also means some trips even see an improvement in travel time, the reason for which is interpreted in the next subsection). In addition, trips with longer travel time observing a stronger dispersion implies that long-distance trips may observe more stochasticities in scenarios with lower speed limits.

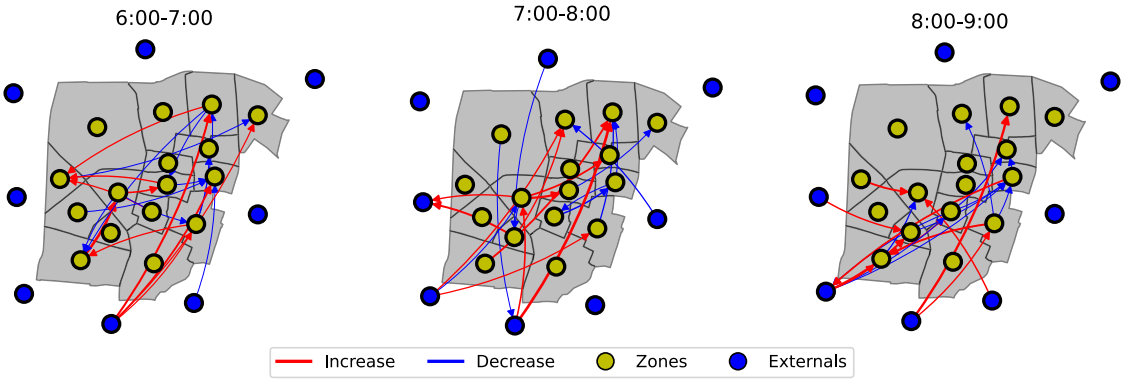

(a) SL40 scenario

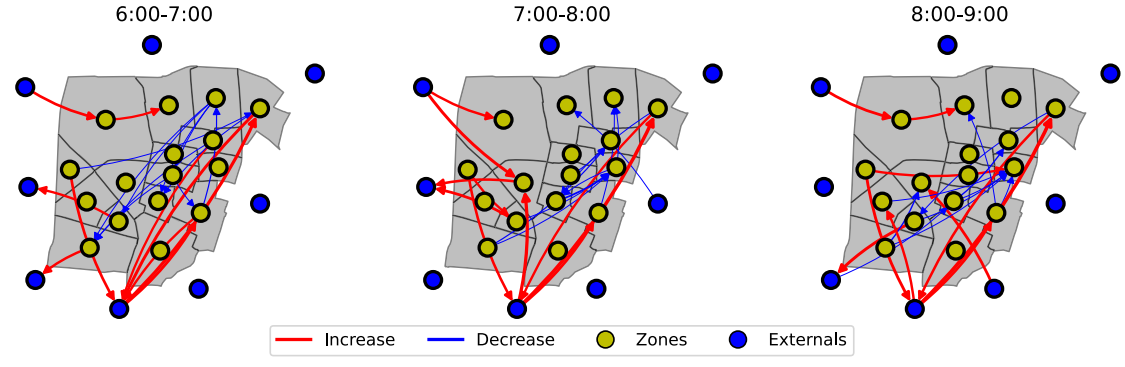

(b) SL30 scenario

Fig. 13. ODs whose travel times are influenced most. (For interpretation of the references to color in this figure legend, the reader is referred to the web version of this article.)

6.4. Changes of OD travel time

It is also important to understand which ODs are affected most and which are affected least such that the policymakers can assess the spatial difference of the potential effect of the policy. Fig. 13 demonstrates the ODs whose travel times are influenced most in the respective scenario. Here we only provide the first 10 ODs that are impeded most (red connections) and the first 10 ODs that are improved most (blue connections). The arrow of the connection annotates the direction of OD, and the width represents the absolute percentage value (the wider the larger). As mentioned in the previous subsection, long-distance (long-time) trips are more likely to change their paths to adapt to the posted speed limits. The main reasons include: (1) Long-distance trips have more route options; (2) Speed limits are mainly posted on the links within the residential area. By counting the number of connections to the external zones, we know that the trips from/to the external zones undertake more impairment in travel time. In SL40, there are 4, 6, and 6 red connections which relate to the external zones in three intervals, respectively. In SL30, they are 9, 9, and 8. In contrast, most blue connections are within the residential area, representing that the implementation of speed limit reduction may even improve the traffic efficiency of some ODs located in the residential area. For the trips within the residential area, shorter secondary links need to travel. With the change in traffic distribution over the network, these trips thus gain the probability of shortening the travel time. Furthermore, the selected ODs vary from different time intervals indicating that the influence on OD travel time is time-dependent. Here temporal dynamics only exist in the demand pattern and demand level. It is beneficial to identify the factors rendering the spatial difference in OD travel time changes. More specifically, we should understand the relationship of the variables from the demand side (e.g., demand pattern) and the supply side (e.g., network structure) with the spatial difference. Assuming one wants to have such a scenario that the travel time changes of some ODs are below a predefined threshold, if the initial scenarios cannot achieve this objective, the estimated relationship model can then be used to tailor the scenario design. This is one potential unit that can be included in the modeling component of the scenario comparison module in Fig. 1.

7. Discussion

This section first introduces a relationship model that can be embedded in the modeling component of the proposed evaluation framework. It models the spatial difference of OD travel time changes with features from the demand model, supply model and

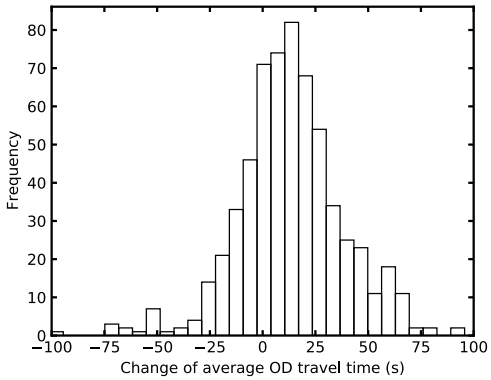

Fig. 14. Distribution of OD travel time changes.

scenario design. Then, the limitation of the risk exposure measurement for pedestrians used in this study is discussed and a method to improve it is provided.

7.1. Understanding the spatial difference of OD travel time changes

To better understand the factors pertaining to the spatial difference of travel time changes, a regression model can be constructed. Features from the supply side mainly include the statistics of objects (i.e., nodes and links) in the network and the metrics for measuring its efficiency (e.g., circuity), connectivity (e.g., node degree, average nearest neighbor degree, clustering coefficient, alpha index, gamma index), centrality (e.g., degree centrality, betweenness centrality,) and complexity (e.g., beta index). It is worth emphasizing that the statistics of target links are explicitly calculated considering they are directly influenced by the speed limit scenario. Features of both the origin TAZ subnetwork and the destination TAZ subnetwork (denote as G_O and G_D, respectively) are constructed. Features from the demand side mainly include the OD demand, OD distance and the number of routes connecting the OD. More importantly, the speed limit scenario that leads to the occurrence of changes is also included in the features set. Each observation in the regression model represents one instance of the OD travel time change. As such, theoretically, it generates 16 (TAZs) × 16 (TAZs) × 3 (intervals) × 2 (scenarios) = 1536 observations. To make the regression model reliable, the observations with less than 5 trips demand are discarded. This process finally leads to 40 independent variables and 612 observations in total. The dependent variable is the OD travel time change, and the independent variables include the variables described above.

Fig. 14 presents the distribution of the dependent variable. It approximately follows a Gaussian distribution with a zero mean. The skewness and kurtosis of this distribution are −0.64 and 6.28, respectively, which are within the respective accepted range recommended by Schminder et al. (2010), i.e., [−2,2] and [−9,9]. So, it is appropriate to apply the Original Least Squares (OLS) regression to estimate the relationship.

The recursive feature elimination (RFE) procedure is used to select significant features based on the p-value (95% confidence level). Then, highly correlated variables are empirically considered and removed from the pruned set. The coefficients for 16 features that are finally employed are given in Appendix for the reader's convenience. Considering the study area is about 5 km × 5 km, the coefficient of OD distance, 0.003, is relatively small, as it means a one-km longer OD distance may only contribute to a three-second increase in the OD travel time. One potential reason is aggregating trips based on the TAZ eliminates the finer OD-dependent changes of individual trips. To this end, one can perform a regression on the change of individual travel time to explore a more precise relation between them. Clearly, the characteristics of both G_O and G_D are significant. However, the influence might be different or even contrary. For example, the estimated coefficient for the average circuity of G_O is −70.619, while the estimated coefficient for that of G_D is 310.911. Another interesting point is the number of intersections in G_D has a negative impact on the increase of OD travel time. The reason could be more intersections provide the probability of finely changing the paths to cross blocks within the residential area. Furthermore, the speed limit is significant with a coefficient of −0.772, indicating that a 10 km/h reduction in speed limit could lead to an increase of about 7.72 s in OD travel time on average.

Fig. 15 demonstrates the difference between the true values and the estimated values by the OLS regression model. In Fig. 15(a), the x-axis is the true value and the y-axis is the estimated value. In Fig. 15(b), the x-axis is the order of observations, while the y-axis is the residual. The location of observations from different scenarios in Fig. 15(a) validates the negative coefficient for the speed limit, i.e., the lower the speed limit is the larger the change of travel time is obtained. The data points are concentrating on the diagonal line with a relatively similar number of samples on the left side and the right side. This is approved by the residual plot in Fig. 15(b). All residuals are fairly located around the $y = 0$ horizontal line, and the number of points on both sides is not significantly different. However, the residuals of SL40 are more compact, implying that the regression model performs better in milder speed limit scenarios.

Note that, here we just provide an example solution for this problem which should be the baseline method. Whereas, one can apply other advanced models to tackle this task for the purpose of attaining the best-fitted result.

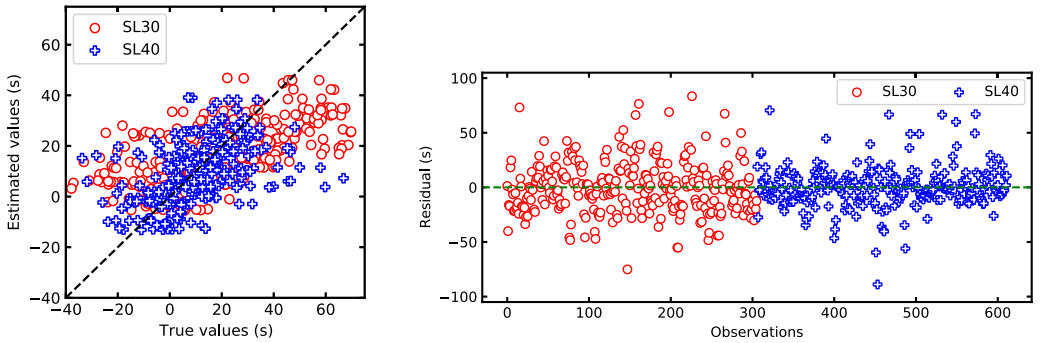

(a) True values vs. estimated values (b) Residuals

Fig. 15. Comparison of true and estimated travel time changes.

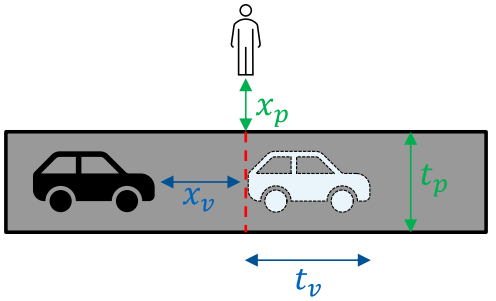

Fig. 16. The conflict between a vehicle and a pedestrian.

Lane 1: $\mathrm{P}_1 = \mathrm{P}(x_v + t_v \geq x_p, x_v \leq t_p + x_p)$
Lane 2: $\mathrm{P}_2 = (1-\mathrm{P}_1)\mathrm{P}\left(x_v + t_v \geq x_p + t_p, x_v \leq 2t_p + x_p\right) = (1-\mathrm{P}_1)\mathrm{P}_1$
⋮ ⋮
Lane n: $\mathrm{P}_n = (1-\mathrm{P}_{n-1})\mathrm{P}_{n-1}$

Fig. 17. Probability of a pedestrian encounters an accident at different lanes.

7.2. A statistical model for measuring risk exposure for pedestrians

Recall that in the evaluation of the risk exposure for pedestrians at the network level, values of the Routledge indicator of links are weighted by the traffic volume. Rigorously speaking, the values should be weighted by the number of pedestrians. Due to the lack of pedestrian data, we make an approximation by assuming links are equally crowded for both pedestrians and vehicles. For those who have pedestrian data, a statistical model is more reliable compared to the relatively rough Routledge indicator. Cameron (1982) develops a statistical model to estimate the exposure and accident risk for pedestrians, where the scenario with pedestrian priority and with vehicle priority are separately modeled. Here we improve it by considering the pedestrian arrival and vehicle arrival simultaneously.

Let the exposure E be the number of potential accidents occurring in a given period T with stationary pedestrian and vehicle arrival rates (λ_p and λ_v, respectively). Fig. 16 illustrates the potential conflict between a vehicle and a pedestrian. The time intervals for pedestrians and vehicles are x_p and x_v, respectively. The time for a pedestrian to cross a lane and the time for a vehicle to pass the cross-section are t_p and t_v. We assume the arrival of pedestrians (X_p) and vehicles (X_v) follow multiple independent Poisson processes. Then the probability density function (PDF) for this process is

$$f_{X_p,X_v}(x_p, x_v) = \lambda_p \lambda_v e^{-\lambda_p x_p - \lambda_v x_v} \tag{13}$$

Hence, the probabilities of the nth pedestrian encountering an accident in different lanes are calculated as shown Fig. 17.

Denote the nth pedestrian suffers an accident as event A_n. $A_n = 1$ indicates an accident happened, while $A_n = 0$ means no accident happened. The probability of $A_n = 1$ is

$$P(A_n = 1) = \sum_{i=1}^{n_l} P_i \tag{14}$$

Therefore, the expectation (denote as Ex) of the exposure in T is calculated as

$$\mathrm{Ex}(E) = \mathrm{Ex}(A_n)(\lambda_v + \lambda_p)T = P(A_n = 1)(\lambda_v + \lambda_p)T \tag{15}$$

The proposed statistical model can improve the evaluation reliability of the risk exposure of crossing. For the one who has relevant data and seeks a more accurate estimation, it is preferable and should replace the Routledge indicator in the evaluation framework.

8. Conclusions

Speed limit policies can render essential and complicated consequences on the traffic flow of an urban network. Considering they are widely adopted as a control measure, appropriate tools for comprehensive quantitative assessments are urgently needed. However, existing works either focus on their function on the target links (i.e., partially investigating its influence from a local perspective), incompletely measure the network-wide effect, or roughly evaluate the impacts based on the urban economy.

In this paper, we develop a systematic simulation-based framework to evaluate speed limit policies. The framework accounts for modeling the effects as per road safety (pedestrian risk and driving safety), traffic efficiency (OD travel time), and the environment (fuel consumption, exhaust emissions, and noise exposure). It contains a four-level comparison system (i.e., network level, link level, route level, and OD level), which makes the evaluation framework hierarchical and systematic. The strength of this framework comes from modeling all different aspects, which are affected by traffic-related policies, where now different global criterion methods can be adapted to combine effects from all the KPIs upon common criteria. Statistical models can be developed between the modeled KPIs and simulation parameters, which provide a more detailed understanding of their correlations. These models can then be directly utilized for either policymaking or optimizing new policy scenarios. The proposed framework is extendable for the assessment of any traffic-related policy and to make the evaluation general, no specific objective is imposed, which can be easily added as per requirement.

Using the proposed framework, we perform a comprehensive evaluation of imposing speed limits to a part of the Munich city center area (Maxvorstadt and Schwabing). Multiple speed limit scenarios are designed by setting identical lower speed limits for all road types (i.e., primary, secondary, and tertiary). The results show that: (i) Speed limit reduction can enhance road safety and the environment within the affected network/area with the cost to traffic efficiency (network level); (ii) Tightening speed limits can contribute to not only the harmonization of traffic flow of the target links but also the traffic flow over the network, represented by the more concentrating distribution for the KPIs (e.g., speed) (link level); (iii) Long-time trips are more likely to change the route choice under low-speed limit scenarios. The influence intensity of reducing the speed limit on the group changing routes and the group not changing routes are distinctive, and the divergence becomes more obvious under stricter speed limits (route level); (iv) The travel between the outer area and the residential area suffers more impairment in travel time, while some travels inside the residential area can even observe an improvement (OD level). According to the insights into the effect of speed limits found in the Munich case study, we recommend the following speed limit policies to reduce the traffic external effects in urban areas.

(1) Implementation of slow zones in urban areas with high population density. To mitigate the traffic external effects around urban residential areas, we recommend piloting slow zones with speed limits set at 30 km/h or lower (e.g., 25 km/h) on all types of roads within the area. While special speed limits for school zones and work zones have already been implemented in Europe (European Commision, 2023) and the USA (FHWA, 2017), the implementation of slow zones in high-density urban areas may also yield significant benefits by reducing traffic externalities.
(2) Enhanced enforcement. Implementing slow zones in a wide variety of road types will require improved compliance levels among drivers and assurance of the effectiveness of slow zone settings. Therefore, it is essential to enhance enforcement measures with lower tolerances. Mannering (2009) and NHTSA (2020) revealed that drivers' perceptions of safe speed are influenced by their expectations of the penalties (even a small amount) incurred for exceeding the speed limit. By implementing stricter enforcement practices, including increased monitoring, and lower tolerance thresholds (more cases but a small amount each), compliance rates can be improved, leading to greater public acceptance of the new policies. This is particularly crucial during the initial stages of implementation. The importance of compliance is also illustrated in Fig. 9.
(3) Microscopic simulation adoption. Instead of relying solely on the conventional approach of using the 85th percentile speed as the speed limit for a given road, we recommend adopting a microscopic simulation-based evaluation method for determining appropriate speed limits. Microscopic simulations provide a comprehensive and area-wide analysis of different speed limit scenarios, modeling detailed traffic, safety and emissions metrics and enabling policymakers to make informed decisions. To facilitate this process, it is recommended that relevant government agencies structure and provide training and resources for adopting microscopic simulation techniques for planning and policy-making.

Table 4
Evaluation of the regression model.

Variables	Coefficient	Description
Intercept	215.966**	Constant
Speed limit	−0.772***	The posted speed limit (km/h)
Variables from the demand side		
OD demand	0.113	Number of trips
OD distance	0.003***	The Haversine distance between OD centroids (m)
Variables from the supply side		
# of nodes in G_O	−0.204***	Number of nodes
Average # of streets to a node	−49.966***	
Average circuity of G_O	−70.619**	Circuity is the total length of links divided by the sum of Euclidean distances between link endpoints.
$\bar{C}$ of G_O	110.975***	Network average clustering coefficient (Clustering coefficient is the ratio of the number of edges between a node and its neighbors to the maximum number of edges that could possibly exist between them.)
Average node degree of G_D	−105.948***	Node degree is the number of links connected to the node.
Average length of links of G_D	−1.009***	
Average # of streets to a node	−30.436**	
# of intersections in G_D	−0.4**	
Average circuity of G_D	310.911***	
$\bar{k}$ of G_D	228.391***	Mean of all average neighbor degrees in the network (The average neighborhood degree of a node is the ratio of the sum of the degree of all neighbor nodes to the degree of itself)
$\bar{C}$ of G_D	302.749***	Network average clustering coefficient
m_s of G_D	0.793**	Number of target links with speed limit
Beta index of G_D	−52.974***	Beta index is the number of links divided by the number of nodes
Model evaluation		
# of observations	612	
R^2	0.259	
R^2_{adj}	0.24	
F-statistic	13.85	

Note: *p < 0.1; **p < 0.05; ***p < 0.01.

We also discuss two methods related to the components present in the proposed evaluation framework. First is an example unit of the modeling component, where an OLS regression model is estimated for low-speed limit scenarios that describe the relationships between change in OD travel times and the features of the demand and supply models. The second method is a statistical model to improve the estimation of risk exposure for pedestrians where the problem is modeled as multiple independent Poisson processes. The model requires information for vehicle and pedestrian arrival, and thus it is not applied in this paper due to the lack of pedestrian data.

This study is subject to certain limitations that should be taken into consideration. Firstly, it relies on the assumption, as discussed in Section 7.2, that both pedestrian and vehicle distributions are evenly spread along the corresponding roads. This assumption may oversimplify the real-world distribution patterns, potentially affecting the accuracy of the results. Secondly, a Wiedemann-99 model calibrated with the traffic data collected at a secondary road is used to simulate driver behaviors within the study area without distinguishing between motorway traffic and interrupted traffic (urban traffic with controlled intersections). While our previous study (Dinar, 2020) has demonstrated that the calibrated Wiedemann-99 model can effectively reproduce urban traffic, it is advisable to employ distinct calibrated driving behavior models for different road types in other cities or areas where relevant data are available. Thirdly, this study focuses solely on car traffic within the study area, excluding the presence of trucks. However, it is important to acknowledge that in some cities, residential areas (consisting of multiple types of roads) may experience traffic flows consisting of both cars and trucks. Given the inherent differences in driving patterns between car and truck drivers, as well as variations in vehicle characteristics, the inclusion of trucks could significantly influence the evaluation of traffic externalities.

For future works, it would be beneficial to construct more units for the modeling component to better explore the relationships between the inputs and the variables of interest. Meanwhile, another interesting direction is to incorporate a controller module to dynamically supervise the development of optimal scenarios by feedback from the scenario evaluation. Accordingly, a network-wide variable speed limit control strategy that focuses on the regional impact for a specific objective (could be multi-objective) can be devised. However, this may be only applicable in the era of CAVs where vehicles get automated network information hence strictly obeying the traffic rules.

CRediT authorship contribution statement

Qing-Long Lu: Conceptualization, Methodology, Software, Formal analysis, Investigation, Visualization, Writing – original draft. **Moeid Qurashi:** Conceptualization, Methodology, Formal analysis, Investigation, Writing – original draft, Writing – review & editing. **Constantinos Antoniou:** Conceptualization, Methodology, Formal analysis, Writing – review & editing, Supervision, Funding acquisition.

Acknowledgments

This research was supported by the European Union's Horizon 2020 i-DREAMS project (Project Number: 814761) funded by European Commission under the MG-2-1-2018 Research and Innovation Action (RIA), and by the CONCERT-Japan DARUMA project (Grant Number: 01DR21010) funded by the German Federal Ministry of Education and Research (BMBF).

Appendix. OLS regression results

See Table 4.

References

Amador, L., Willis, C.J., 2014. Demonstrating a correlation between the maturity of road safety practices and road safety incidents. Traffic Inj. Prev. 15 (6), 591–597.

Anil Chaudhari, A., Srinivasan, K.K., Rama Chilukuri, B., Treiber, M., Okhrin, O., 2022. Calibrating wiedemann-99 model parameters to trajectory data of mixed vehicular traffic. Transp. Res. Rec. 2676 (1), 718–735.

Ashfaq, M., Gu, Z., Waller, S.T., Saberi, M., 2021. Comparing dynamic user equilibrium and noniterative stochastic route choice in a simulation-based dynamic traffic assignment model: Practical considerations for large-scale networks. J. Adv. Transp. 2021.

Banks, G., 2010. Evidence-based policy making: What is it? How do we get it? In: World Scientific Reference on Asia-Pacific Trade Policies: 2: Agricultural and Manufacturing Protection in Australia. World Scientific, pp. 719–736.

Cameron, M.H., 1982. A method of measuring exposure to pedestrian accident risk. Accid. Anal. Prev. 14 (5), 397–405.

De Pauw, E., Daniels, S., Thierie, M., Brijs, T., 2014. Safety effects of reducing the speed limit from 90 km/h to 70 km/h. Accid. Anal. Prev. 62, 426–431.

Delhaye, E., 2006. Traffic safety: speed limits, strict liability and a km tax. Transp. Res. A 40 (3), 205–226.

Di Costanzo, L., Coppola, A., Pariota, L., Petrillo, A., Santini, S., Bifulco, G.N., 2020. Variable speed limits system: A simulation-based case study in the city of naples. In: 2020 IEEE International Conference on Environment and Electrical Engineering and 2020 IEEE Industrial and Commercial Power Systems Europe. pp. 1–6.

Dinar, Y., 2020. Impact of Connected and/or Autonomous Vehicles in Mixed Traffic (Master Thesis). Technical University of Munich, Munich.

Erdmann, J., 2015. Sumo's lane-changing model. In: Modeling Mobility with Open Data. Springer, pp. 105–123.

European Commision, 2023. Current speed limit policies. https://road-safety.transport.ec.europa.eu/eu-road-safety-policy/priorities/safe-road-use/safe-speed/archive/current-speed-limit-policies (Last accessed on 2023-05-19).

Farrag, S., El-Hansali, M.Y., Yasar, A., Shakshuki, E.M., 2020. Simulation-based evaluation of using variable speed limit in traffic incidents. Procedia Comput. Sci. 175, 340–348.

FHWA, 2017. Speed limit basics. https://highways.dot.gov/safety/speed-management/speed-limit-basics (Last accessed on 2023-05-19).

Fildes, B., Lawrence, B., Oxley, J., 2019. Low speed limits in residential areas in Melbourne, Australia. Traffic Inj. Prev. 20 (sup2), S155–S157.

Greenshields, B., Bibbins, J., Channing, W., Miller, H., 1935. A study of traffic capacity. In: Highway Research Board Proceedings, Vol. 1935. National Research Council (USA), Highway Research Board.

Grumert, E., Ma, X., Tapani, A., 2015. Analysis of a cooperative variable speed limit system using microscopic traffic simulation. Transp. Res. C 52, 173–186.

Hallenbeck, M.E., Ishimaru, J., Nee, J., et al., 2003. Measurement of Recurring Versus Non-Recurring Congestion. Technical Report, Washington (State) Department of Transportation.

Hensher, D.A., 2006. Integrating accident and travel delay externalities in an urban speed reduction context. Transp. Rev. 26 (4), 521–534.

Howarth, C., Routledge, D., Repetto-Wright, R., 1974. An analysis of road accidents involving child pedestrians. Ergonomics 17 (3), 319–330.

Infras, A.G., 2010. Handbuch für emissionsfaktoren des strassenverkehrs (version 3.1). https://www.hbefa.net/e/index.html (Last accessed on 2021-08-19).

Islam, M.T., El-Basyouny, K., 2015. Full Bayesian evaluation of the safety effects of reducing the posted speed limit in urban residential area. Accid. Anal. Prev. 80, 18–25.

Jo, Y., Choi, H., Jeon, S., Jung, I., 2012. Variable speed limit to improve safety near traffic congestion on urban freeways. In: 2012 IEEE International Conference on Information Science and Technology. IEEE, pp. 43–50.

Krajzewicz, D., Behrisch, M., Wagner, P., Luz, R., Krumnow, M., 2015. Second generation of pollutant emission models for SUMO. In: Modeling Mobility with Open Data. Springer, pp. 203–221.

Lan, Z., Cai, M., 2021. Dynamic traffic noise maps based on noise monitoring and traffic speed data. Transp. Res. D 94, 102796.

Lasley, P., 2021. 2021 Urban Mobility Report. Technical Report, Texas A&M Transportation Institute.

Lassarre, S., Papadimitriou, E., Yannis, G., Golias, J., 2007. Measuring accident risk exposure for pedestrians in different micro-environments. Accid. Anal. Prev. 39 (6), 1226–1238.

Lopez, P.A., Behrisch, M., Bieker-Walz, L., Erdmann, J., Flötteröd, Y.-P., Hilbrich, R., Lücken, L., Rummel, J., Wagner, P., Wießner, E., 2018. Microscopic traffic simulation using sumo. In: 2018 21st International Conference on Intelligent Transportation Systems. ITSC, IEEE, pp. 2575–2582.

Lu, X.-Y., Varaiya, P., Horowitz, R., Su, D., Shladover, S.E., 2011. Novel freeway traffic control with variable speed limit and coordinated ramp metering. Transp. Res. Rec. 2229 (1), 55–65.

Madireddy, M., De Coensel, B., Can, A., Degraeuwe, B., Beusen, B., De Vlieger, I., Botteldooren, D., 2011. Assessment of the impact of speed limit reduction and traffic signal coordination on vehicle emissions using an integrated approach. Transp. Res. D 16 (7), 504–508.

Makarewicz, R., Kokowski, P., 2007. Prediction of noise changes due to traffic speed control. J. Acoust. Soc. Am. 122 (4), 2074–2081.

Mannering, F., 2009. An empirical analysis of driver perceptions of the relationship between speed limits and safety. Transp. Res. F 12 (2), 99–106.

Nezafat, R.V., Beheshtitabar, E., Cetin, M., Williams, E., List, G.F., 2018. Modeling and evaluating traffic flow at sag curves when imposing variable speed limits on connected vehicles. Transp. Res. Rec.: J. Transp. Res. Board 2672 (20), 193–202.

NHTSA, 2020. Speed limits | NHTSA. https://www.nhtsa.gov/book/countermeasures/countermeasures/11-speed-limits (Last accessed on 2023-05-19).

Nitzsche, E., Tscharaktschiew, S., 2013. Efficiency of speed limits in cities: A spatial computable general equilibrium assessment. Transp. Res. A 56, 23–48.

Nota, R., Barelds, R., van Maercke, D., 2005. Harmonoise WP 3 engineering method for road traffic and railway noise after validation and fine-tuning. In: Deliverable of WP3 of the HARMONOISE Project. Document ID HAR32TR-040922-DGMR20.

Onelcin, P., Alver, Y., 2017. The crossing speed and safety margin of pedestrians at signalized intersections. Transp. Res. Procedia 22, 3–12.

Papadoulis, A., Quddus, M., Imprialou, M., 2019. Evaluating the safety impact of connected and autonomous vehicles on motorways. Accid. Anal. Prev. 124, 12–22.

Qurashi, M., Lu, Q.-L., Cantelmo, G., Antoniou, C., 2022. Dynamic demand estimation on large scale networks using principal component analysis: The case of non-existent or irrelevant historical estimates. Transp. Res. C 136, 103504.

Renski, H., Khattak, A.J., Council, F.M., 1999. Effect of speed limit increases on crash injury severity: analysis of single-vehicle crashes on north carolina interstate highways. Transp. Res. Rec. 1665 (1), 100–108.
Routledge, D., Repetto-Wright, R., Howarth, C., 1974a. A comparison of interviews and observation to obtain measures of children's exposure to risk as pedestrians. Ergonomics 17 (5), 623–638.
Routledge, D., Repetto-Wright, R., Howarth, C., 1974b. The exposure of young children to accident risk as pedestrians. Ergonomics 17 (4), 457–480.
Sadat, M., Celikoglu, H.B., 2017. Simulation-based variable speed limit systems modelling: An overview and a case study on Istanbul freeways. Transp. Res. Procedia 22, 607–614.
Schminder, E., Ziegler, M., Danay, E., Beyer, L., Bühner, M., 2010. Is it really robust? Reinvestigating the robustness of ANOVA against violations of the normal distribution. Eur. Res. J. Methods Behav. Soc. Sci. 6 (4), 147–151.
Slavik, R., Gnap, J., 2020. Speed and noise as a problem of safety in residential areas. In: 2020 XII International Science-Technical Conference Automotive Safety. IEEE, Kielce, Poland, pp. 1–8.
Soriguera, F., Torné, J.M., Rosas, D., 2013. Assessment of dynamic speed limit management on metropolitan freeways. J. Intell. Transp. Syst. 17 (1), 78–90.
Spall, J.C., 1998. Implementation of the simultaneous perturbation algorithm for stochastic optimization. IEEE Trans. Aerosp. Electron. Syst. 34 (3), 817–823.
Sun, F., Dubey, A., White, J., 2017. DxNAT—Deep neural networks for explaining non-recurring traffic congestion. In: 2017 IEEE International Conference on Big Data (Big Data). IEEE, pp. 2141–2150.
Tscharaktschiew, S., 2020. Why are highway speed limits really justified? An equilibrium speed choice analysis. Transp. Res. B 138, 317–351.
Vadeby, A., Forsman, Å., 2018. Traffic safety effects of new speed limits in Sweden. Accid. Anal. Prev. 114, 34–39.
van Benthem, A., 2015. What is the optimal speed limit on freeways? J. Public Econ. 124, 44–62.
Wardrop, J.G., 1952. Road paper. some theoretical aspects of road traffic research. Proc. Inst. Civ. Eng. 1 (3), 325–362.
Wiedemann, R., Reiter, U., 1992. Microscopic traffic simulation: the simulation system MISSION, background and actual state. In: Project ICARUS (V1052) Final Report, Vol. 2. pp. 1–53.
You, J., Fang, S., Zhang, L., Taplin, J., Guo, J., 2018. Enhancing freeway safety through intervening in traffic flow dynamics based on variable speed limit control. J. Adv. Transp. 2018, 1–10.
Zhang, Y., Ioannou, P.A., 2016. Combined variable speed limit and lane change control for highway traffic. IEEE Trans. Intell. Transp. Syst. 18 (7), 1812–1823.
Zhang, J., Wu, K., Cheng, M., Yang, M., Cheng, Y., Li, S., 2020. Safety evaluation for connected and autonomous vehicles' exclusive lanes considering penetrate ratios and impact of trucks using surrogate safety measures. J. Adv. Transp. 2020.
Zhao, P., Chapman, R., Randal, E., Howden-Chapman, P., 2013. Understanding resilient urban futures: a systemic modelling approach. Sustainability 5 (7), 3202–3223.